Assigning chemoreceptors to chemosensory pathways in *Pseudomonas aeruginosa*

Davi R. Ortega[a,1], Aaron D. Fleetwood[b,c,1,2], Tino Krell[d], Caroline S. Harwood[e], Grant J. Jensen[a,f], and Igor B. Zhulin (Игорь Жулин)[b,c,3]

[a]Department of Biology and Biological Engineering, California Institute of Technology, Pasadena, CA 91125; [b]Computational Sciences and Engineering Division, Oak Ridge National Laboratory, Oak Ridge, TN 37831; [c]Department of Microbiology, University of Tennessee, Knoxville, TN 37996; [d]Department of Environmental Protection, Estación Experimental del Zaidín, Consejo Superior de Investigaciones Científicas, 18008 Granada, Spain; [e]Department of Microbiology, University of Washington, Seattle, WA 98195; and [f]Howard Hughes Medical Institute, California Institute of Technology, Pasadena, CA 91125

Edited by Eugene V. Koonin, National Institutes of Health, Bethesda, MD, and approved October 26, 2017 (received for review May 27, 2017)

In contrast to *Escherichia coli*, a model organism for chemotaxis that has 5 chemoreceptors and a single chemosensory pathway, *Pseudomonas aeruginosa* PAO1 has a much more complex chemosensory network, which consists of 26 chemoreceptors feeding into four chemosensory pathways. While several chemoreceptors were rigorously linked to specific pathways in a series of experimental studies, for most of them this information is not available. Thus, we addressed the problem computationally. Protein–protein interaction network prediction, coexpression data mining, and phylogenetic profiling all produced incomplete and uncertain assignments of chemoreceptors to pathways. However, comparative sequence analysis specifically targeting chemoreceptor regions involved in pathway interactions revealed conserved sequence patterns that enabled us to unambiguously link all 26 chemoreceptors to four pathways. Placing computational evidence in the context of experimental data allowed us to conclude that three chemosensory pathways in *P. aeruginosa* utilize one chemoreceptor per pathway, whereas the fourth pathway, which is the main system controlling chemotaxis, utilizes the other 23 chemoreceptors. Our results show that while only a very few amino acid positions in receptors, kinases, and adaptors determine their pathway specificity, assigning receptors to pathways computationally is possible. This requires substantial knowledge about interacting partners on a molecular level and focusing comparative sequence analysis on the pathway-specific regions. This general principle should be applicable to resolving many other receptor–pathway interactions.

signal transduction | protein–protein interactions | chemotaxis | computational prediction

The microorganism *Pseudomonas aeruginosa* is ubiquitous and the leading cause of nosocomial infections (1). It exhibits two types of motility, swimming and twitching, which are powered by flagellar motors and type IV pili (TFP), respectively. Both types of motility are controlled by chemosensory pathways and both are necessary for efficient host colonization and virulence (2). The interference with motility and chemotaxis was proposed as a strategy to block infection (3).

The chemosensory pathway controlling motility is best understood in *Escherichia coli*: it consists of five chemoreceptors that detect signals and relay information to CheA histidine kinase via a CheW adaptor protein. The signal is then transmitted to flagellar motors via a CheY response regulator, which is phosphorylated by CheA. The pathway also involves two adaptation enzymes, CheB methylesterase and CheR methyltransferase, which change the methylation state of the chemoreceptors, and CheZ phosphatase, which de-phosphorylates CheY (4, 5).

In contrast to *E. coli*, more bacterial species have multiple chemosensory systems that control not only motility but also other cellular functions, and they have a correspondingly larger number of chemoreceptors (6–8). In *Rhodobacter sphaeroides*, a model system for complex chemosensory pathways (9), only 3 chemoreceptors of 11 have been rigorously linked to specific pathways (10, 11), indicating that resolving their connectivity is difficult. Chemosensing in *P. aeruginosa* PAO1 is even more complicated. There are four chemosensory pathways that are encoded by five gene clusters. Cluster I and cluster V encode proteins that form the Che I pathway (Table S1), which is essential for chemotaxis (12). According to the evolutionary classification scheme, this cluster belongs to class F6 (where letter F followed by the class number, 1–17, denotes pathways controlling flagella-mediated motility) (8). Cluster II encodes proteins of the Che II pathway, which is required for an optimal chemotactic response (13) and virulence (14) and belongs to class F7 (8). Che I/F6 and Che II/F7 pathway proteins localize to the cell pole, but at separate subcellular locations (15). Cluster II genes are expressed in the stationary phase of growth, and all but *mcpA* are quorum-regulated (16). Cluster III encodes the Wsp pathway (9), which regulates biofilm formation by stimulating c-di-GMP synthesis (6) and belongs to the evolutionary class ACF (alternative cellular functions) (8). The Wsp signaling complex is localized not only at the poles, but also around the periphery of cells (17, 18). Finally, the Chp pathway, which is formed by products of cluster IV, controls twitching motility (19), and causes alterations in the cAMP levels (20); it belongs to the evolutionary class TFP (8).

P. aeruginosa PAO1 has 26 chemoreceptors that feed into these pathways (Table S1). Four of them are present in chemotaxis gene clusters: cluster II contains *mcpA* and *mcpB* and the *chp* and *wsp* clusters contain *pilJ* and *wspA*, correspondingly. The remaining 22 chemoreceptor genes are scattered over the genome. PilJ and WspA were rigorously and unambiguously demonstrated to be part of the Chp (19–23) and Wsp (17, 18, 24)

Significance

Multiple receptors transmit information to several signaling pathways that control cellular functions. Which receptor feeds into which pathway and what defines the receptor/pathway specificity are the key questions in cell biology. Here we show that in a model bacterium receptor/pathway specificity is determined by small motifs that can be revealed by comparative sequence analysis of receptor regions that interact with the pathway components. This study provides a path toward computational assignment of receptors to their respective cellular pathways in thousands of bacterial genomes.

Author contributions: D.R.O., A.D.F., and I.B.Z. designed research; D.R.O. and A.D.F. performed research; D.R.O. contributed new reagents/analytic tools; D.R.O., A.D.F., T.K., C.S.H., G.J.J., and I.B.Z. analyzed data; and D.R.O., A.D.F., T.K., C.S.H., G.J.J., and I.B.Z. wrote the paper.

The authors declare no conflict of interest.

This article is a PNAS Direct Submission.

[1]D.R.O. and A.D.F. contributed equally to this work.

[2]Present address: College of Medicine, University of Tennessee Health Sciences Center, Memphis, TN 38163.

[3]To whom correspondence should be addressed. Email: ijouline@utk.edu.

This article contains supporting information online at www.pnas.org/lookup/suppl/doi:10.1073/pnas.1708842114/-/DCSupplemental.

pathways, correspondingly. Ten chemoreceptors—PctA, PctB, PctC (25, 26), CtpH, CtpL (27, 28), TlpQ (29), McpA (30), PA2652 (31), McpS (32), and McpK (33)—were implicated in chemotaxis. However, there is only limited experimental evidence that permits their assignment to the major (Che I/F6) chemotaxis pathway. Interestingly, while *mcpA* and *mcpB* are both found in the *che II* gene cluster, once expressed, McpB colocalizes with the Che II/F7 pathway, as expected, but McpA colocalizes with Che I/F6 (15). Finally, for 10 *P. aeruginosa* PAO1 chemoreceptors there are no data regarding their potential association with any of the four chemosensory pathways.

We apply several computational approaches to link each of the *P. aeruginosa* chemoreceptors to their respective signal transduction pathways and show that where chemoreceptors have been assigned to a pathway experimentally, they match computational predictions obtained by analyzing pathway-specific chemoreceptor regions.

Results

General Computational Approaches to Predict Protein–Protein Interactions. First, all chemoreceptors were subjected to automated searches against the STRING database (34): the results are shown in Dataset S1. In each case, predicted interacting partners were components of chemosensory pathways, indicating the overall reliability of the method; however, unambiguous assignments to a single pathway could be made only for PilJ and WspA. Next, we extracted sequences of CheA, adaptors and chemoreceptors from complete *Pseudomonadales* genomes from the MiST database (35) and organized them in clusters of orthologous groups (COGs) (36), as previously described (37) (Dataset S2). The presence and absence of each COG was mapped to a phylogenetic tree of *Pseudomonadales* (Fig. S1). Based on these results, we can assign only one chemoreceptor, PilJ, to the corresponding Chp/TFP system. An interesting feature revealed by phylogenetic profiling is the apparent coevolution of McpA and the F7 and F8 pathways (Fig. S1). McpA is encoded in gene neighborhoods of F8 and F7 pathways, thus supporting its association with the Che II/F7 pathway.

Only 4 of the 26 *P. aeruginosa* PAO1 chemoreceptors are encoded within chemosensory gene clusters (Table S1). In search for coexpression data for chemoreceptors and pathway components, we mined a rich transcriptomic compendium for *P. aeruginosa*, which provides integration of expression data from more than 100 independent experiments (38). We looked for appearances of all chemotaxis genes with high potential coregulation (Fig. S2). The data strongly support coexpression of *pilJ* and the rest of the *chp*/TFP gene cluster and coexpression of *mcpK* and the *che I*/F6 cluster; however, data for other chemoreceptor genes was inconclusive.

Specificity Between Chemoreceptor and Pathway Classes. Chemoreceptors can be classified in terms of the number of helical heptads that comprise their conserved signaling domain (39). For example, the *E. coli* chemoreceptor Tsr has 36 heptads in its signaling domain (Fig. 1) and thus belongs to the 36H class. Genomic evidence suggested that chemoreceptors of certain heptad classes interact preferentially with certain chemosensory pathway classes defined based on evolutionary considerations (8). We revisited this relationship by identifying 403 complete genomes in the MiST database (35) that had a single chemosensory pathway and assigned all chemoreceptors in these genomes to their pathways (8, 39). Our analysis confirmed previously found patterns, but it also revealed that chemoreceptors from certain classes, for example 24H and 40H, are associated with pathways that belong to various classes (Table S2). Conversely, pathways that belong to the same class (e.g., F6) can be associated with chemoreceptors from different heptad classes. We classified all 1,724 chemoreceptors from the 81 complete *Pseudomonadales* genomes in four heptad classes: 40H (82%), 24H (7%), 36H (2%), and 34H (1%) (with 8% unclassified). In the *P. aeruginosa* PAO1 genome, 21 chemoreceptors were classified as 40H, 2 as 24H, 1 as 36H, and 2 remained unclassified (Table S1). Because three of the four chemosensory pathways (Che I/F6, Wsp/ACF, Chp/TFP) in *P. aeruginosa* potentially can utilize the majority of chemoreceptors in the genome (40H class), their pathway assignment cannot be clarified. However, the only 36H class chemoreceptor can be confidently assigned to the Che II/F7 pathway, because 36H chemoreceptors were never found in genomes containing F6 as the sole chemosensory pathway and 40H chemoreceptors are not associated with F7 pathways (Table S2).

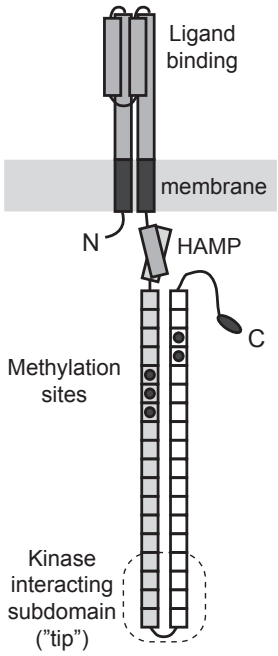

Fig. 1. Cartoon representation of the *E. coli* chemoreceptor Tsr. One subunit of the native homodimer is depicted. The cytoplasmic portion below the HAMP domain comprises a signaling domain, which is composed of 36 helical heptads: 18 in its N-terminal part shown in gray and 18 in its C-terminal part shown in white. The hairpin tip of the signaling domain contains regions responsible for interaction with kinase CheA and adaptor CheW. Methylation sites shown as black circles are located in heptads N14, N15, N16, C19, and C20. Chemoreceptor heptad nomenclature is according to Alexander and Zhulin (39). Tsr lacks heptads N5, N6, N17, N18, C5, C6, C17, and C18.

Pathway-Specific Signaling Complex Patterns. In a chemosensory complex, chemoreceptors interact with the kinase, adaptors and each other via a distinct, highly conserved subdomain known as the tip (Fig. 1). These multifaceted interactions are the likely reason for the unusually high sequence conservation in the tip (39, 40). However, we hypothesized that there should be variations in the pattern that lead to pathway specificity. To identify these variations, we built consensus sequences for each of the chemoreceptor COGs and then compared them using hierarchical clustering and conserved sequence pattern visualization. The clustering/pattern visualization revealed a motif (LLAxxxxIExAR), which is identical in 23 chemoreceptor COGs, but is different in 3 other chemoreceptor COGs: McpB (ILAxxxxVExAR), WspA (LLSxxxxIExEK), and PilJ (ILAxxxxIQxSM) (Fig. 2).

Experimental studies identified likely chemoreceptor-CheA (41–43) and chemoreceptor-CheW (42, 44, 45) binding determinants in homologous systems from *Thermotoga maritima* and *E. coli*. We mapped these sites on the corresponding positions of *Pseudomonas* chemoreceptors and found that, satisfactorily, they overlap with the pathway-specificity motif (Fig. 2). If indeed the specificity determinants on chemoreceptors overlap with CheA and CheW binding sites, then the opposite should also be true: regions in CheA and CheW that contain chemoreceptor-binding

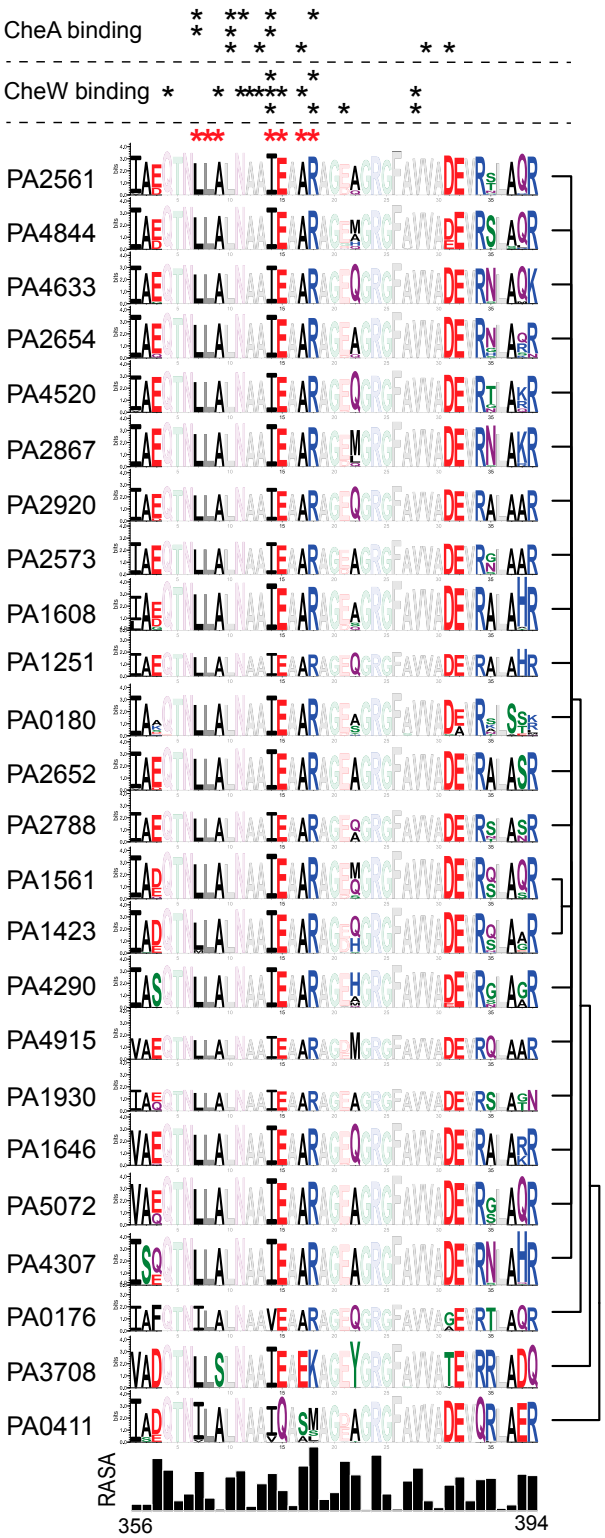

Fig. 2. Conservation patterns of the kinase/adaptor binding subdomain in *P. aeruginosa* chemoreceptors. Sequence logos ordered by clustering based on similarity of consensus sequences of each chemoreceptor COG. The relative accessible surface area (RASA) calculated based on the Tsr crystal structure (PDB ID code 1QU7) is shown below to reveal the exposed residues. Structural similarity and extreme sequence conservation in the chemoreceptor tip (39, 40) suggest that such extrapolation is feasible. Residues that are part of the motif defining chemoreceptor specificity are marked with red asterisks above the logos. The experimentally determined CheA [*Top* three rows, data obtained by crystallography (42), NMR (41), and disulfide mapping (43)] and CheW [*Bottom* three rows, data obtained by crystallography (42), NMR (44), and disulfide mapping (45)] binding sites are marked with black asterisks. Residue numbers are given for positions in TM1413 chemoreceptor from *T. maritima* (correspond to positions 371–409 in Tsr).

sites should contain specificity determinants. To verify this proposition, we used multiple sequence alignments of CheA COGs to map chemoreceptor binding sites identified in homologous systems (Fig. 3*A* and Dataset S3). Conservation patterns revealed a motif clearly distinguishing the four CheA histidine kinases in *P. aeruginosa*: LTYIVES in PA1458 (F6), LVNVNEI in PA0178 (F7), LAHIERM in PA3704 (ACF), and LNTIEGI in PA0413 (TFP). Similarly to the binding sites on chemoreceptors, the CheA motifs consist of positions that are universally conserved between all homologs and positions that are uniquely conserved in each CheA class (i.e., are pathway-specific). Fig. 3*B* shows visualization of some of the potential pathway-specific contacts between a chemoreceptor and CheA using the all-atom model of the *T. maritima* chemosensory array (46).

The four chemosensory pathways in *P. aeruginosa* utilize eight adaptor-like proteins, each belonging to a unique COG. COG assignments (Dataset S2), phylogenetic trees (Fig. S3), and gene neighborhood associations (Table S1) allowed us to assign each adaptor-like protein to a specific pathway. We mapped experimentally determined CheW chemoreceptor-binding sites on consensus sequences of adaptor proteins (Fig. 3 *C* and *D*). Similarly to CheA, the majority of these sites mapped to a small region of the CheW domain around a highly conserved residue E38 (numbering for *E. coli* CheW protein), which forms a salt bridge with R62 to maintain the correct alignment of the chemoreceptor and kinase binding sites of CheW (47). Remarkably, the overall sequence similarity comparison places CheW proteins from F6 (PA1464) and F7 (PA0177) pathways together, whereas CheV is placed into a separate cluster (Fig. S3); however, the identified chemoreceptor-specificity motif is shared by CheW-F6 and CheV (NVxxVxEVL), but it is quite different in CheW-F7 (DIxxVxEIR) (Fig. 3*C*). Both CheW-F6 (PA1464) and CheV are known to be part of the same signaling pathway in *P. aeruginosa* (Table S1), thus supporting the specificity-motif assignment. In addition, we found that seven adaptor proteins contain the conserved E38-R62 salt bridge, whereas it is missing from the CheW-domain containing protein PA1463 (Fig. S3). Consequently, we propose that this protein is not involved in chemosensing, but acts similarly to the CheW domain-containing ParP protein from *Vibrio cholerae* (48).

Pathway-Specific Conserved Methylation Sites. Experimental studies showed that the CheR methyltransferases in *P. aeruginosa* and *Pseudomonas putida* are pathway-specific (49, 50). CheR methylates specific glutamyl residues that are well conserved (39). We have identified one putative methylation site (Fig. 4*A* and Dataset S4) that was conserved not only in sequence, but also in its location on a specific heptad C13, in 19 chemoreceptors (all from 40H class) that we assigned to the Che I/F6 pathway. From all of the 26 chemoreceptors in the genome, 4 did not have any identifiable methylation sites and may undergo methylation-independent adaptation similarly to the Aer chemoreceptor in *E. coli* (51): McpA, BdlA, PA4290, and McpS. In a remarkable contrast, WspA and PilJ had predicted methylation sites that were differently conserved in sequence and were found in different heptads (C14 and C15, respectively). In McpB, which was predicted to interact with the Che II/F7 pathway, the methylation site pattern is nearly identical to that of the Tsr chemoreceptor, which belongs to the F7 chemosensory pathway in *E. coli* (Fig. 4*A* and Fig. S3).

All CheR methyltransferases contain an N-terminal domain, which is proposed to interact with the methylation regions in chemoreceptors. Furthermore, several positively charged amino

MICROBIOLOGY

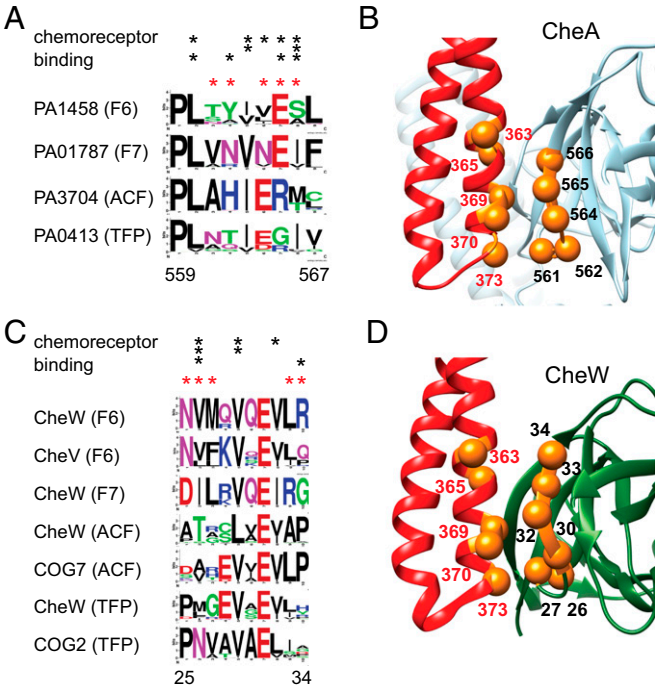

Fig. 3. Conservation patterns in the chemoreceptor-binding region of *P. aeruginosa* kinases and adaptors. (*A*) Sequence logos of consensus sequences of CheA kinases from four chemosensory pathways. Residue numbers are given for corresponding positions in CheA from *T. maritima*. The experimentally determined chemoreceptor-binding sites are marked with black asterisks, where rows from *Top* to *Bottom* show data obtained by crystallography (42), NMR (41), and disulfide mapping (43). Residues that are part of the motif defining kinase specificity are marked with red asterisks above the logos. (*B*) Mapping of the specificity defining motif residues (shown in gold) on the chemoreceptor (in red)–kinase (in blue) interaction surface modeled using crystal structures of signaling complex components and electron cryotomography of *T. maritima* chemosensory arrays (46). (*C*) Sequence logos of consensus sequences of the adaptor protein region implicated in chemoreceptor binding. Residue numbers are given for corresponding positions in the *T. maritima* CheW protein. Experimentally determined binding sites are marked with black asterisks, where rows from *Top* to *Bottom* show data obtained by crystallography (42), NMR (44), and disulfide mapping (45). Residues that are part of the motif defining adaptor specificity are marked with red asterisks above the logos. (*D*) Mapping of the specificity defining motif residues (shown in gold) on the chemoreceptor (in red)–CheW (in green) interaction surface modeled using crystal structures of signaling complex components and electron cryotomography of *T. maritima* chemosensory arrays (46).

acid residues in the second α-helix of this domain were cross-linked with negatively charged residues on the surface of the methylation region (52). Conservation patterns of CheR COGs show expected enrichment with positively charged residues, but at the same time, their locations are strikingly different in CheR proteins from different pathways (Fig. 4*B*), thus complementing the presence of pathway-specificity determinants in the chemoreceptor methylation regions.

Based on several lines of evidence derived by independent computational approaches and taking into consideration a large volume of published experimental data, we were able to assign each of the 26 chemoreceptors in *P. aeruginosa* PAO1 to a single chemosensory pathway (Fig. 5).

Discussion

Assigning receptors to different pathways is a combinatorial problem, which worsens with increasing numbers in each category. With its 26 chemoreceptors possibly working with four individual pathways, *P. aeruginosa* PAO1 presents a challenging case. We addressed the problem computationally and used available experimental data

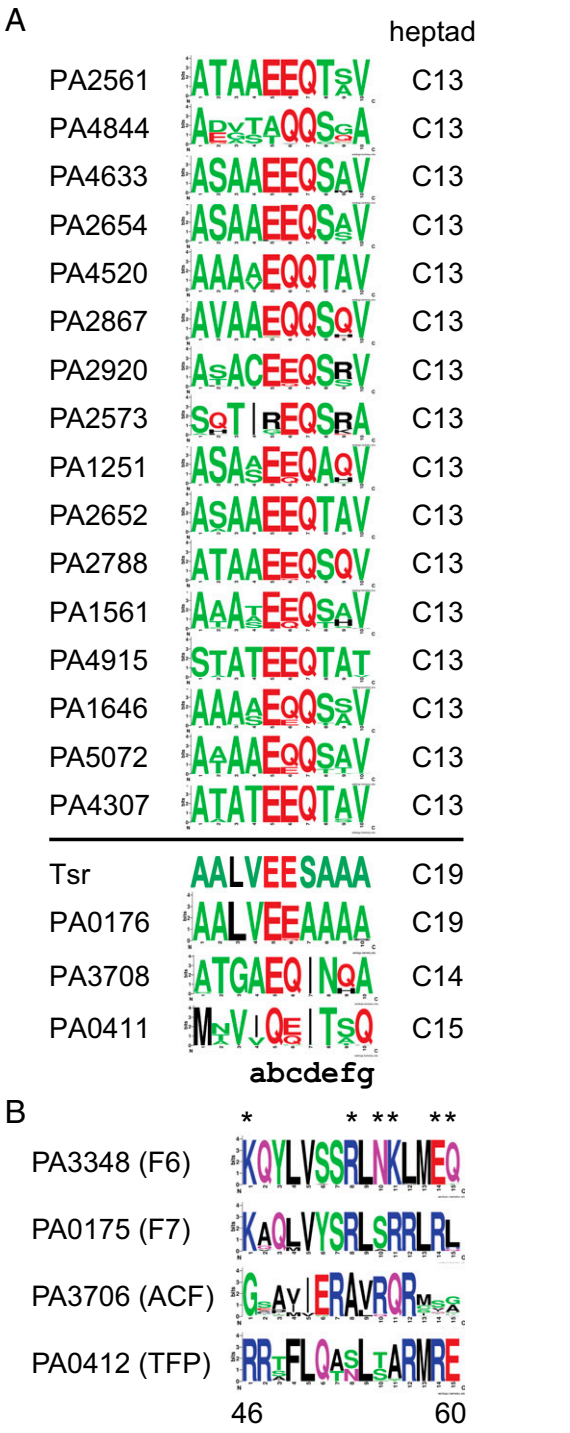

Fig. 4. Conservation of the predicted methylation site in the C terminus of *P. aeruginosa* chemoreceptors. (*A*) Sequence logos derived from multiple sequence alignments of chemoreceptor COGs and heptad positions of the corresponding methylation site are shown. Glu and Gln residues are shown in red, small residues are shown in green, and large residues are shown in black. Corresponding region from the *E. coli* chemoreceptor Tsr is shown for comparison above the consensus logo for *Pseudomonas* McpB orthologs that belong to the same heptad class, 36H. (*B*) Sequence logos of consensus sequences of the CheR region implicated in binding to the chemoreceptor methylation regions. Residue numbers are given for corresponding positions in the *E. coli* CheR. Experimentally determined binding sites (52) are marked with black asterisks.

to design more focused computational inquiries. Explicitly, the key information for assigning chemoreceptors to individual pathways came from comparative sequence analysis of their specific regions that are involved in protein–protein interactions: conserved methylation sites and the CheA kinase/CheW adaptor-interacting subdomain. Subsequently, we were able to assign each chemoreceptor to an individual pathway. Three chemosensory pathways in *P. aeruginosa* utilize only one dedicated chemoreceptor, whereas the fourth pathway, which is the main system controlling chemotaxis, utilizes 23 chemoreceptors.

Satisfactorily, available experimental data match pertinent assignments, making credible other assignments for which no experimental data are currently available. The computational prediction that McpB is the sole chemoreceptor interacting with the Che II/F7 chemotaxis pathway is in full agreement with published experimental evidence. No Che II/F7 chemosensory complex formation occurs in the *mcpB* mutant, indicating that the absence of this chemoreceptor cannot be compensated by the presence of other receptors (15). This is further supported by the fact that the CheR methyltransferase of the Che II/F7 pathway exclusively methylates McpB (49).

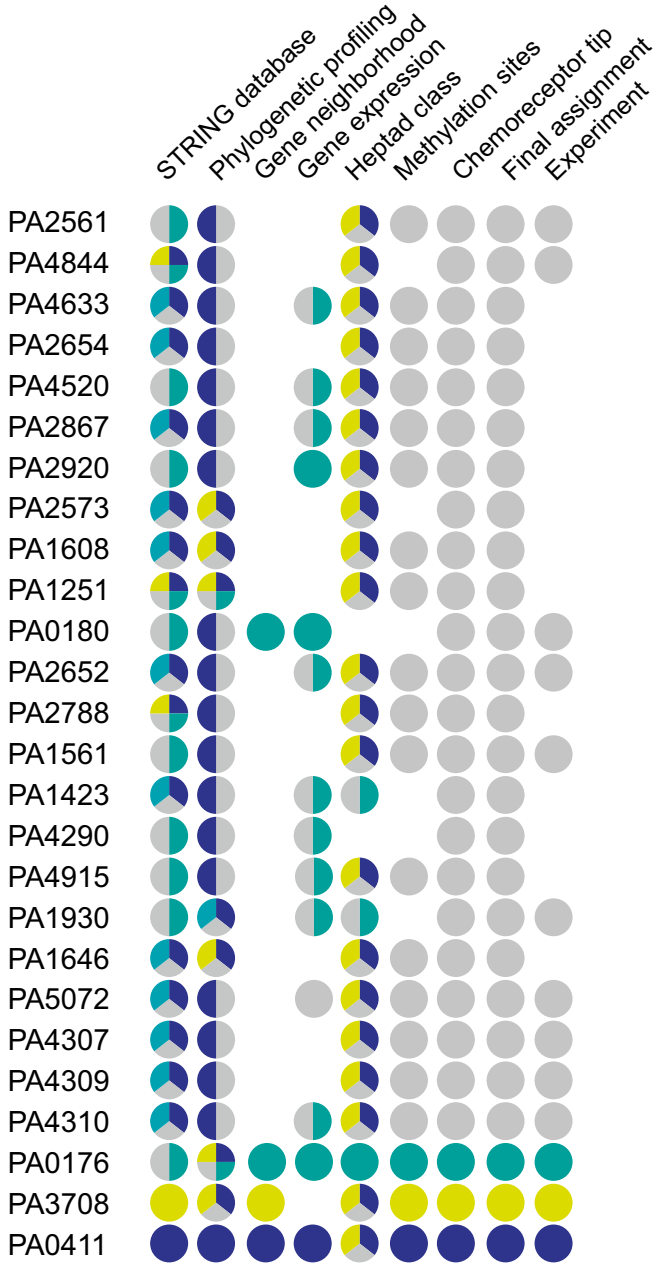

Fig. 5. Assignment of chemoreceptors to pathways based on multiple evidence. Pathway assignment: Chp/TFP, blue; Wsp/ACF, yellow; Che I/F6, gray; Che II/F7, green.

The computational prediction that WspA is the sole receptor interacting with the Wsp pathway is also in full agreement with available experimental evidence. WspA is absolutely required for c-di-GMP formation by the response regulator WspR (17, 18, 24). Computational prediction that PilJ is the sole chemoreceptor interacting with the Chp/TFP pathway also agrees with previously published experimental evidence. The deletion of *pilJ* results in loss of surface piliation, twitching motility, and reduction in cAMP levels (19–23) that are all controlled by the Chp/TFP pathway.

Computational prediction that 23 other chemoreceptors in *P. aeruginosa* PAO1 all feed into a single Che I/F6 pathway, which is the major system controlling chemotaxis (12), is supported by a significant body of experimental evidence implicating several of these chemoreceptors, namely PctA, PctB, and PctC (25, 26), CtpH and CtpL (27, 28), TlpQ (29), McpA (30), PA2652 (31), McpS (32), and McpK (33) in chemotaxis. However, experimental evidence alone cannot exclude a possibility that some or all of these chemoreceptors can potentially interact with the Che II/F7 pathway, which is also involved in mediating chemotaxis. Our computational results argue strongly against this possibility. Furthermore, for all other chemoreceptors in *P. aeruginosa*, experimental evidence is lacking and the results of the computational analyses presented here enable assignment of these chemoreceptors to the major chemotaxis pathway.

One case that appears to contradict our prediction involves the BdlA chemoreceptor, which we assign to the major (F6) chemotaxis pathway based on the conservation of the signaling domain. A substantial body of experimental evidence links BdlA to biofilm formation and c-di-GMP turnover (53, 54), functions that are also attributed to the Wsp/ACF chemosensory pathway; however, there are no data suggesting that BdlA feeds into this pathway. BdlA was shown to interact with two c-di-GMP–modulating enzymes, DipA and GcbA (55, 56), that are not connected to any of the four chemosensory pathways. More importantly, BdlA has never been studied in chemotaxis assays and, in contrast to DipA and RbdA, chemotaxis proteins were not subjected to pull-down assays with BdlA. Thus, our prediction that BdlA interacts with the main chemotaxis pathway awaits experimental verification.

One of the strongest advantages of comparative genomic analysis is its ability not only to uncover, but also to refute certain relationships. This is much harder to do experimentally. For example, while experimental evidence that WspA specifically interacts with the Wsp pathway is overwhelming, one cannot exclude the possibility that one or more other chemoreceptors might interact with the same pathway. In this case, WspA has unique sequence patterns in two regions where it interacts with the Wsp pathway (methylation sites and kinase/adaptor binding subdomain); all of the other chemoreceptors have very different sequence patterns. Thus, no other chemoreceptor than WspA is predicted to interact with the Wsp pathway.

On the other hand, without in-depth a priori knowledge about these biological pathways obtained through various experimental approaches by many research groups over decades, most of our computational analyses would not work, as clearly illustrated by failed attempts to solve the problem using general bioinformatics approaches.

Methods

Sequences of chemotaxis proteins and associated information were obtained from the MiST 2.2 database (35). Standard bioinformatics tools and packages were used in all computational approaches (see *SI Methods* for full details).

ACKNOWLEDGMENTS. We thank Jacob Pollack for technical assistance and Ariane Briegel for helpful discussions. This work was supported in part by National Institutes of Health Grants GM072295 (to I.B.Z.) and GM122588 (to G.J.J.).

1. Lyczak JB, Cannon CL, Pier GB (2000) Establishment of *Pseudomonas aeruginosa* infection: Lessons from a versatile opportunist. *Microbes Infect* 2:1051–1060.
2. Kazmierczak BI, Schniederberend M, Jain R (2015) Cross-regulation of *Pseudomonas* motility systems: The intimate relationship between flagella, pili and virulence. *Curr Opin Microbiol* 28:78–82.
3. Erhardt M (2016) Strategies to block bacterial pathogenesis by interference with motility and chemotaxis. *Curr Top Microbiol Immunol* 398:185–205.
4. Parkinson JS, Hazelbauer GL, Falke JJ (2015) Signaling and sensory adaptation in *Escherichia coli* chemoreceptors: 2015 update. *Trends Microbiol* 23:257–266.
5. Wadhams GH, Armitage JP (2004) Making sense of it all: Bacterial chemotaxis. *Nat Rev Mol Cell Biol* 5:1024–1037.
6. Hickman JW, Tifrea DF, Harwood CS (2005) A chemosensory system that regulates biofilm formation through modulation of cyclic diguanylate levels. *Proc Natl Acad Sci USA* 102:14422–14427.
7. Zusman DR, Scott AE, Yang Z, Kirby JR (2007) Chemosensory pathways, motility and development in *Myxococcus xanthus*. *Nat Rev Microbiol* 5:862–872.
8. Wuichet K, Zhulin IB (2010) Origins and diversification of a complex signal transduction system in prokaryotes. *Sci Signal* 3:ra50.
9. Porter SL, Wadhams GH, Armitage JP (2011) Signal processing in complex chemotaxis pathways. *Nat Rev Microbiol* 9:153–165.
10. Wadhams GH, Martin AC, Armitage JP (2000) Identification and localization of a methyl-accepting chemotaxis protein in *Rhodobacter sphaeroides*. *Mol Microbiol* 36: 1222–1233.
11. Wadhams GH, et al. (2002) TlpC, a novel chemotaxis protein in *Rhodobacter sphaeroides*, localizes to a discrete region in the cytoplasm. *Mol Microbiol* 46: 1211–1221.
12. Kato J, Nakamura T, Kuroda A, Ohtake H (1999) Cloning and characterization of chemotaxis genes in *Pseudomonas aeruginosa*. *Biosci Biotechnol Biochem* 63: 155–161.
13. Ferrández A, Hawkins AC, Summerfield DT, Harwood CS (2002) Cluster II che genes from *Pseudomonas aeruginosa* are required for an optimal chemotactic response. *J Bacteriol* 184:4374–4383.
14. Garvis S, et al. (2009) *Caenorhabditis elegans* semi-automated liquid screen reveals a specialized role for the chemotaxis gene *cheB2* in *Pseudomonas aeruginosa* virulence. *PLoS Pathog* 5:e1000540.
15. Güvener ZT, Tifrea DF, Harwood CS (2006) Two different *Pseudomonas aeruginosa* chemosensory signal transduction complexes localize to cell poles and form and remould in stationary phase. *Mol Microbiol* 61:106–118.
16. Schuster M, Hawkins AC, Harwood CS, Greenberg EP (2004) *The Pseudomonas aeruginosa* RpoS regulon and its relationship to quorum sensing. *Mol Microbiol* 51: 973–985.
17. Güvener ZT, Harwood CS (2007) Subcellular location characteristics of the *Pseudomonas aeruginosa* GGDEF protein, WspR, indicate that it produces cyclic-di-GMP in response to growth on surfaces. *Mol Microbiol* 66:1459–1473.
18. O'Connor JR, Kuwada NJ, Huangyutitham V, Wiggins PA, Harwood CS (2012) Surface sensing and lateral subcellular localization of WspA, the receptor in a chemosensory-like system leading to c-di-GMP production. *Mol Microbiol* 86:720–729.
19. Whitchurch CB, et al. (2004) Characterization of a complex chemosensory signal transduction system which controls twitching motility in *Pseudomonas aeruginosa*. *Mol Microbiol* 52:873–893.
20. Fulcher NB, Holliday PM, Klem E, Cann MJ, Wolfgang MC (2010) The *Pseudomonas aeruginosa* Chp chemosensory system regulates intracellular cAMP levels by modulating adenylate cyclase activity. *Mol Microbiol* 76:889–904.
21. Darzins A (1994) Characterization of a *Pseudomonas aeruginosa* gene cluster involved in pilus biosynthesis and twitching motility: Sequence similarity to the chemotaxis proteins of enterics and the gliding bacterium *Myxococcus xanthus*. *Mol Microbiol* 11: 137–153.
22. DeLange PA, Collins TL, Pierce GE, Robinson JB (2007) PilJ localizes to cell poles and is required for type IV pilus extension in *Pseudomonas aeruginosa*. *Curr Microbiol* 55: 389–395.
23. Luo Y, et al. (2015) A hierarchical cascade of second messengers regulates *Pseudomonas aeruginosa* surface behaviors. *MBio* 6:e02456–e14.
24. Huangyutitham V, Güvener ZT, Harwood CS (2013) Subcellular clustering of the phosphorylated WspR response regulator protein stimulates its diguanylate cyclase activity. *MBio* 4:e00242–e13.
25. Taguchi K, Fukutomi H, Kuroda A, Kato J, Ohtake H (1997) Genetic identification of chemotactic transducers for amino acids in *Pseudomonas aeruginosa*. *Microbiology* 143:3223–3229.
26. Rico-Jiménez M, et al. (2013) Paralogous chemoreceptors mediate chemotaxis towards protein amino acids and the non-protein amino acid gamma-aminobutyrate (GABA). *Mol Microbiol* 88:1230–1243.
27. Wu H, et al. (2000) Identification and characterization of two chemotactic transducers for inorganic phosphate in *Pseudomonas aeruginosa*. *J Bacteriol* 182:3400–3404.
28. Rico-Jiménez M, et al. (2016) Two different mechanisms mediate chemotaxis to inorganic phosphate in *Pseudomonas aeruginosa*. *Sci Rep* 6:28967.
29. Kim H-E, Shitashiro M, Kuroda A, Takiguchi N, Kato J (2007) Ethylene chemotaxis in *Pseudomonas aeruginosa* and other *Pseudomonas* species. *Microbes Environ* 22: 186–189.
30. Kim HE, et al. (2006) Identification and characterization of the chemotactic transducer in *Pseudomonas aeruginosa* PAO1 for positive chemotaxis to trichloroethylene. *J Bacteriol* 188:6700–6702.
31. Alvarez-Ortega C, Harwood CS (2007) Identification of a malate chemoreceptor in *Pseudomonas aeruginosa* by screening for chemotaxis defects in an energy taxis-deficient mutant. *Appl Environ Microbiol* 73:7793–7795.
32. Bardy SL, Maddock JR (2005) Polar localization of a soluble methyl-accepting protein of *Pseudomonas aeruginosa*. *J Bacteriol* 187:7840–7844.
33. Martín-Mora D, et al. (2016) Identification of a chemoreceptor in *Pseudomonas aeruginosa* that specifically mediates chemotaxis toward α-ketoglutarate. *Front Microbiol* 7:1937.
34. Franceschini A, et al. (2013) STRING v9.1: Protein-protein interaction networks, with increased coverage and integration. *Nucleic Acids Res* 41:D808–D815.
35. Ulrich LE, Zhulin IB (2010) The MiST2 database: A comprehensive genomics resource on microbial signal transduction. *Nucleic Acids Res* 38:D401–D407.
36. Tatusov RL, Koonin EV, Lipman DJ (1997) A genomic perspective on protein families. *Science* 278:631–637.
37. Ortega DR, Zhulin IB (2016) Evolutionary genomics suggests that CheV Is an additional adaptor for accommodating specific chemoreceptors within the chemotaxis signaling complex. *PLoS Comput Biol* 12:e1004723.
38. Tan J, Hammond JH, Hogan DA, Greene CS (2016) ADAGE-based integration of publicly available *Pseudomonas aeruginosa* gene expression data with denoising autoencoders iluminates microbe-host interactions. *mSystems* 1:e00025-15.
39. Alexander RP, Zhulin IB (2007) Evolutionary genomics reveals conserved structural determinants of signaling and adaptation in microbial chemoreceptors. *Proc Natl Acad Sci USA* 104:2885–2890.
40. Ortega DR, et al. (2013) A phenylalanine rotameric switch for signal-state control in bacterial chemoreceptors. *Nat Commun* 4:2881.
41. Wang X, Vu A, Lee K, Dahlquist FW (2012) CheA-receptor interaction sites in bacterial chemotaxis. *J Mol Biol* 422:282–290.
42. Li X, et al. (2013) The 3.2 Å resolution structure of a receptor: CheA:CheW signaling complex defines overlapping binding sites and key residue interactions within bacterial chemosensory arrays. *Biochemistry* 52:3852–3865.
43. Piasta KN, Ulliman CJ, Slivka PF, Crane BR, Falke JJ (2013) Defining a key receptor-CheA kinase contact and elucidating its function in the membrane-bound bacterial chemosensory array: A disulfide mapping and TAM-IDS study. *Biochemistry* 52: 3866–3880.
44. Vu A, Wang X, Zhou H, Dahlquist FW (2012) The receptor-CheW binding interface in bacterial chemotaxis. *J Mol Biol* 415:759–767.
45. Pedetta A, Parkinson JS, Studdert CA (2014) Signalling-dependent interactions between the kinase-coupling protein CheW and chemoreceptors in living cells. *Mol Microbiol* 93:1144–1155.
46. Cassidy CK, et al. (2015) CryoEM and computer simulations reveal a novel kinase conformational switch in bacterial chemotaxis signaling. *eLife* 4:e08419.
47. Ortega DR, et al. (2013) Conformational coupling between receptor and kinase binding sites through a conserved salt bridge in a signaling complex scaffold protein. *PLoS Comput Biol* 9:e1003337.
48. Ringgaard S, et al. (2014) ParP prevents dissociation of CheA from chemotactic signaling arrays and tethers them to a polar anchor. *Proc Natl Acad Sci USA* 111: E255–E264.
49. García-Fontana C, Corral Lugo A, Krell T (2014) Specificity of the CheR2 methyltransferase in *Pseudomonas aeruginosa* is directed by a C-terminal pentapeptide in the McpB chemoreceptor. *Sci Signal* 7:ra34.
50. García-Fontana C, et al. (2013) High specificity in CheR methyltransferase function: CheR2 of *Pseudomonas putida* is essential for chemotaxis, whereas CheR1 is involved in biofilm formation. *J Biol Chem* 288:18987–18999.
51. Bibikov SI, Miller AC, Gosink KK, Parkinson JS (2004) Methylation-independent aerotaxis mediated by the *Escherichia coli* Aer protein. *J Bacteriol* 186:3730–3737.
52. Shiomi D, Zhulin IB, Homma M, Kawagishi I (2002) Dual recognition of the bacterial chemoreceptor by chemotaxis-specific domains of the CheR methyltransferase. *J Biol Chem* 277:42325–42333.
53. Morgan R, Kohn S, Hwang SH, Hassett DJ, Sauer K (2006) BdlA, a chemotaxis regulator essential for biofilm dispersion in *Pseudomonas aeruginosa*. *J Bacteriol* 188: 7335–7343.
54. Petrova OE, Sauer K (2012) Dispersion by *Pseudomonas aeruginosa* requires an unusual posttranslational modification of BdlA. *Proc Natl Acad Sci USA* 109: 16690–16695.
55. Petrova OE, Sauer K (2012) PAS domain residues and prosthetic group involved in BdlA-dependent dispersion response by *Pseudomonas aeruginosa* biofilms. *J Bacteriol* 194:5817–5828.
56. Petrova OE, Cherny KE, Sauer K (2015) The diguanylate cyclase GcbA facilitates *Pseudomonas aeruginosa* biofilm dispersion by activating BdlA. *J Bacteriol* 197: 174–187.
57. Katoh K, Toh H (2008) Recent developments in the MAFFT multiple sequence alignment program. *Brief Bioinform* 9:286–298.
58. Stamatakis A (2014) RAxML version 8: A tool for phylogenetic analysis and post-analysis of large phylogenies. *Bioinformatics* 30:1312–1313.
59. Swofford DL (2002) *PAUP*. Phylogenetic Analysis Using Parsimony (*and Other Methods) Version 4* (Sinauer Associates, Sunderland, MA).
60. Crooks GE, Hon G, Chandonia JM, Brenner SE (2004) WebLogo: A sequence logo generator. *Genome Res* 14:1188–1190.
61. Eddy SR (1998) Profile hidden Markov models. *Bioinformatics* 14:755–763.
62. Eddy SR (2011) Accelerated profile HMM searches. *PLoS Comput Biol* 7:e1002195.
63. Ciccarelli FD, et al. (2006) Toward automatic reconstruction of a highly resolved tree of life. *Science* 311:1283–1287.
64. Finn RD, et al. (2014) Pfam: The protein families database. *Nucleic Acids Res* 42: D222–D230.
65. Felsenstein J (1989) PHYLIP–Phylogeny inference package (version 3.2). *Cladistics* 5: 164–166.
66. Humphrey W, Dalke A, Schulten K (1996) VMD: Visual Molecular Dynamics. *J Mol Graph* 14:27–28, 33–38.